2009 American Control Conference
Hyatt Regency Riverfront, St. Louis, MO, USA
June 10-12, 2009

Vehicle Stabilization in Response to Exogenous Impulsive Disturbances to the Vehicle Body

Jing Zhou, Jianbo Lu, and Huei Peng

Abstract—**Road traffic statistics have shown that multi-event crashes typically result in a higher death toll than single-event crashes. One type of those multi-event crashes could be a crash where the initial harmful event leads to a loss of directional control of the vehicle. In this work, we study countermeasures during such crashes, namely, vehicle stabilization in response to exogenous impulsive disturbances. A vehicle collision model is developed to characterize vehicle motions due to a light impact, and a sensing scheme is proposed to detect crash events associated with loss of control afterwards. The stabilization controller, which is developed from the sliding surface control approach, is then activated and attenuates undesired vehicle motions via differential braking/active steering. The effectiveness of the proposed method is verified through CarSim simulations. This vehicle stabilization can be thought as a function extension to existing electronic stability control systems.**

I. Introduction

AUTOMOTIVE safety is of great importance for drivers, manufacturers, government agencies and our society. Significant technological and regulatory efforts have been devoted to promote ground vehicle safety. Generally speaking, the existing safety measures can be categorized into two major fields: active safety for accident prevention and avoidance, as well as passive safety to mitigate the severity of injuries if accidents do occur.

Despite advances in vehicle safety technology, the death toll of road traffic accidents remains steady. According to traffic safety statistics, approximately 6 million motor vehicle traffic crashes were reported to the police during 2006 in the United States [1]. National Automotive Sampling System - Crashworthiness Data System (NASS-CDS) data from 1988 through 2004 show that every year in the US, about 2.9 million light passenger vehicles are involved in tow-away crashes annually. Approximately 31% of these vehicles have at least one additional harmful event following the initial collision. The NASS-CDS data analysis also showed that risks of both injury and fatality increased with the number of collision events. A separate accident statistical study performed by the German Insurance Association confirms that even a vehicle involved in a light impact (e.g., the collisions with impact forces under certain thresholds) is likely to experience a severe secondary crash, and 1/3 of all accidents with severe injuries consist of multiple events [2].

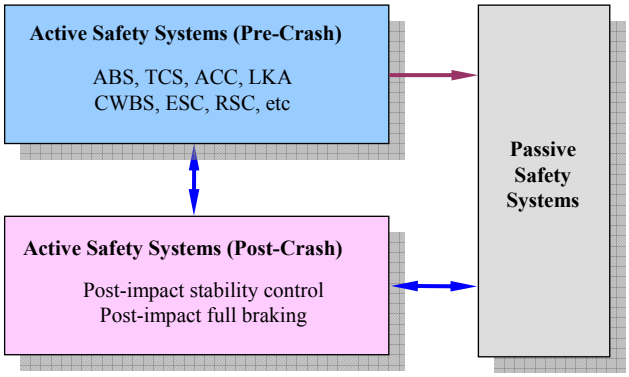

Fig. 1. Concept of the comprehensive vehicle safety system.

Few studies have directly addressed vehicle dynamics control in response to exogenous impulsive disturbances applied to the vehicle body. One prominent example is the study reported by Chan *et al.* [3], in which a steering control system was developed to demonstrate the feasibility of post-impact maneuvers to mitigate accident consequences. A number of collision scenarios were simulated to demonstrate the effectiveness. However, its controller relied on the information about vehicle position in lane and heading angle, which are challenging to retrieve unless a computer vision or a magnetic marker sensing system is installed. Furthermore, the targeted collision scenarios were relatively mild (peak post-impact heading angle < 10°). For collisions with higher severity, steering control alone is probably incapable of stabilizing the vehicle.

In 2007 Bosch released a prototype Secondary Collision Mitigation (SCM) safety feature [4]. The SCM function networks between airbag control system (passive safety) and ESP (active safety). It triggers automatic braking on four wheels (ABS braking) as soon as the airbag-firing criteria are met, so that vehicle speed can be maximally reduced. Since the total kinetic energy decays fast, the tendency of secondary collisions is averted or at least their severity is moderated.

Electronic stability control (ESC) systems have been widely equipped on modern vehicles to provide stability enhancement and handling predictability. They operate by comparing the driver's intent with the vehicle's actual

This work was supported by the Ford Motor Company.

J. Zhou is with the Department of Mechanical Engineering at the Univ. of Michigan, Ann Arbor, Michigan, 48109 (corresponding author, phone: 734-647-9732; e-mail: jzhouz@umich.edu).

J. Lu is with Research & Advanced Engineering at Ford Motor Company, Dearborn, Michigan (e-mail: jlu10@ford.com).

H. Peng is with the Department of Mechanical Engineering at the Univ. of Michigan, Ann Arbor, Michigan (e-mail: hpeng@umich.edu).

responses via measurements of steering wheel angle, lateral acceleration, yaw rate, and wheel rotational velocities. In case of discrepancy, ESC applies selective braking or reduces engine torque to correct possible understeer or oversteer tendency.

A technical assessment of a research ESC system, which mimics the performance of the existing ESC, for post-impact stabilizing purposes was conducted by Thor [5]. Since ESC is designed to stabilize vehicle motions in the event of a mismatch between the vehicle and the driver request due to tire force variations (i.e., the disturbance and the control mechanisms are from the same source – the tire force variations), an exogenous impact induced vehicle motion is likely beyond the operation range of the ESC.

It is of interest to identify the occurrence of exogenous forces imposed on the vehicle leading to loss of control and to apply active yaw control to counteract the loss of control when the ESC does not provide enough counteracting forces. Such strategy is likely to request braking forces that are larger than those normally used in ESC systems so as to quickly attenuate undesired vehicle motions (spin-out, skid, and roll) induced by this initial impact, such that subsequent crashes can be avoided or mitigated. The proposed stabilization system constitutes a small step towards a comprehensive vehicle safety system that consist of conventional active safety systems, post-crash active safety measures, and passive safety systems, along with their interactions (Fig. 1). Such a total safety system expands the operational horizon of active safety systems from preventive measures to post-event mitigation measures, which have previously been the responsibility solely of passive safety devices, such as airbags.

The rest of this paper is organized as follows. Based on a previously-developed collision model to characterize vehicle motions after light impacts, a crash sensing and validation scheme is proposed in Section II to detect potential crash events. The design of a post-impact stability controller based on differential braking and active steering is conducted in Section III. Its effectiveness is demonstrated in angled rear-end collisions simulated with CarSim software in Section IV. Conclusions and future work are outlined in the end.

II. Detection & Validation of Impulsive Disturbances

For the proposed vehicle stabilization system to operate, it has to be activated at the right moment and should not be turned on by faulty measurements, sensor noises or the other non-impact events. A sensing and validation scheme is proposed in this section to address the detection of an impulsive disturbance and the time at which subsequent abnormal and undesired vehicle motion follows.

In this study, yaw rate and lateral acceleration signals are the main decision-making signals used to identify the conditions for system activation. Suppose the sampling time is 0.01 second, which is normally used for the brake control systems. As soon as three continuous large inter-sample changes in yaw rate and lateral acceleration are registered, where the absolute magnitude of the changes is beyond the ranges of changes corresponding a drivers' manual operation, then it is assumed that the vehicle has experienced an intense yaw and lateral motion caused by certain impact that warrants the intervention of the vehicle stabilization system. The sensing thresholds for the gradients of yaw rate and lateral acceleration used in the specific example of this paper are set at $\Delta\omega_z$ = 3 deg/s for yaw rate and ΔA_y = 0.1 g for lateral acceleration between samples, respectively. The choice of the values is based on calibrations with computer simulations.

In practice, an abnormal change in successive samples does not necessarily lead to the conclusion that a crash is occurring, since this symptom may also be caused by sensor defects or accidental noises. In order to eliminate the possibility of improper characterization of an event, the apparent crash event needs to be validated by continuously monitoring key kinematic variables.

The validation procedure of the impulsive disturbance is illustrated in Fig. 2. The actual duration of the crash is from the time instant "O" to "D." This crash is presumably detected at "B" by meeting the above criteria, as a consequence the stabilization system is then active and can be activated. The estimated crash onset is positioned at the time instant "A" since three sampling intervals are used. Then the crash severity and location as well as the predicted vehicle responses at a future time instant "C" are computed, which is five samples downstream from the current time step. When the actual time course reaches the time instant "C," measured yaw rate and lateral velocity are compared with their predicted versions. If there is agreement, the crash event detected at the time instant "B" is validated. Otherwise, the impact event is invalidated and the vehicle stabilization system would be de-activated.

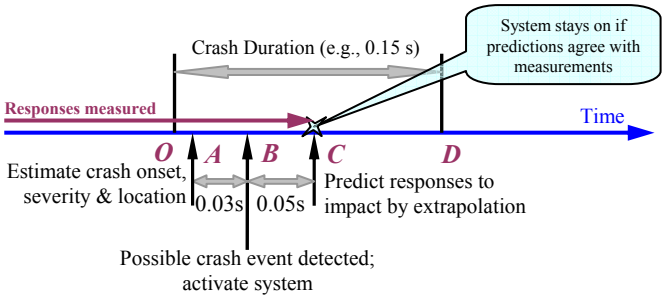

Fig. 2. Illustration of the crash validation procedure.

One critical step in the procedure is to estimate the magnitude and the location of the impulse, given accessible vehicle states and a limited set of nominal vehicle parameters. A previously developed model in [6] for light impacts is applied for this purpose. The components of the impulse (P_x, P_y) and its location (x_A, y_A) are inferred on the basis of Eqs. (1)- (3). If the slip angles of front/rear axles become so large that tire lateral forces reach the adhesion limit, corresponding

terms will be replaced.

$$P_x = M_1 \cdot \left(V_{1x} - v_{1x}\right) - M_1 \frac{\Delta t}{2}\left(V_{1y}\Omega_{1z} + v_{1y}\omega_{1z}\right) \tag{1}$$

$$P_y = M_1 \cdot \left(V_{1y} - v_{1y}\right) + M_1 \frac{\Delta t}{2}\left(V_{1x}\Omega_{1z} + v_{1x}\omega_{1z}\right) - m_{R1}h_1 \cdot \left(\Omega_{1x} - \omega_{1x}\right) + \frac{\Delta t}{2} C_{f1}\left(\frac{V_{1y} + a_1\Omega_{1z}}{V_{1x}} - \frac{v_{1y} + a_1\omega_{1z}}{v_{1x}}\right) + \frac{\Delta t}{2} C_{r1}\left(\frac{V_{1y} - b_1\Omega_{1z}}{V_{1x}} - \frac{v_{1y} - b_1\omega_{1z}}{v_{1x}}\right) \tag{2}$$

$$P_y x_A - P_x y_A = I_{zz1}\left(\Omega_{1z} - \omega_{1z}\right) + I_{xz1}\left(\Omega_{1x} - \omega_{1x}\right) + \frac{\Delta t}{2} a_1 C_{f1}\left(\frac{V_{1y} + a_1\Omega_{1z}}{V_{1x}} - \frac{v_{1y} + a_1\omega_{1z}}{v_{1x}}\right) - \frac{\Delta t}{2} b_1 C_{r1}\left(\frac{V_{1y} - b_1\Omega_{1z}}{V_{1x}} - \frac{v_{1y} - b_1\omega_{1z}}{v_{1x}}\right) \tag{3}$$

Since the envisioned scenario is light collisions without substantial vehicle dimensional changes, the location of the impact is assumed to fall on the vehicle periphery instead of an arbitrary position inside the vehicle. Consequently, when solving for x_A and y_A, two cases (side and rear-end impact assumptions) will be dealt with simultaneously. Only the geometrically realistic answers will be accepted.

A linear extrapolation is used to predict (P_x, P_y) at a future time step, because during the brief interval of an on-going crash, impulses are monotonically increasing values. A short prediction horizon (e.g. 50 ms) will be employed. Based on the difference between the estimated current impulses and the predicted impulses, the magnitude of collision forces within the short prediction horizon can be derived. Then a four-DOF vehicle dynamics model [7] can be used to make projections on vehicle kinematic states at the end of the prediction window, which will be compared with the measurements afterwards to check their agreements and to further verify the occurrence of an impact event.

III. Controller Development

The post-impact stabilization control is approached by treating the struck vehicle with substantial initial conditions induced by the impact and the subsequent efforts to bring it back to the desired states. The control objective is to attenuate sideslip angle, yaw rate, and roll rate as soon as an impulsive crash disturbance is detected, and to recover vehicle stability as quickly as possible.

The following general assumptions are made. First of all, for the proposed control system to operate effectively, the braking and steering systems are assumed to function normally despite the collision, i.e., the impact is a light impact that does not cause severe damage to the vehicle, its components, or subsystems.

Furthermore, the controller is assumed to have access to all the necessary vehicle states, for instance, measured yaw rate, longitudinal velocity, lateral acceleration, as well as estimated lateral velocity, tire forces, and so on. Concerns over practical constraints as well as system robustness against varying road surface conditions and tire force estimation inaccuracy will be explored in the later phase of this research process.

The derivation of the controller is based on a planar two-track three-DOF vehicle model (Fig. 3), without the presence of exogenous forces. If the front steering angle δ is reasonably small, it is straightforward to obtain equations of motion for lateral and yaw dynamics.

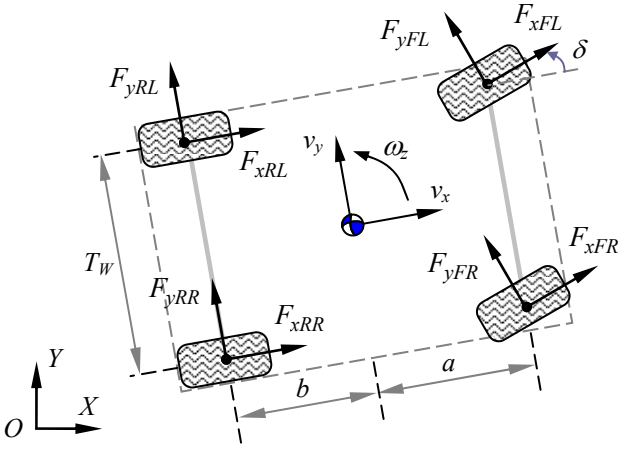

Fig. 3. A planar view of the 3-DOF vehicle model.

$$M \cdot \left(\dot{v}_y + v_x\omega_z\right) = \left(F_{xFL} + F_{xFR}\right)\delta + \left(F_{yFL} + F_{yFR} + F_{yRL} + F_{yRR}\right) \tag{4}$$

$$I_{zz}\dot{\omega}_z = a \cdot \left(F_{yFL} + F_{yFR}\right) - b \cdot \left(F_{yRL} + F_{yRR}\right) + a \cdot \left(F_{xFL} + F_{xFR}\right)\delta + \frac{T_W}{2} \cdot \left[\left(F_{xFR} - F_{xFL}\right) + \left(F_{xRR} - F_{xRL}\right)\right] - \frac{T_W}{2} \cdot \left(F_{yFR} - F_{yFL}\right)\delta \tag{5}$$

The two system states (sideslip velocity and yaw rate) are denoted as $x_1 = v_y$, $x_2 = \omega_z$. When the tire slip angles are small (lower than 6°, depending on tire characteristics), the tire lateral forces can be related to the cornering stiffness [7] and computed with the following

$$F_{yf} = F_{yFL} + F_{yFR} = C_f\left(\delta - \frac{v_y + a\omega_z}{v_x}\right),$$
$$F_{yr} = F_{yRL} + F_{yRR} = C_r\left(-\frac{v_y - b\omega_z}{v_x}\right). \tag{6}$$

The two possible inputs to the system are a yaw moment realized through differential braking forces and a front axle steering angle.

$$u_1 = \frac{T_W}{2} \cdot \left(F_{xFR} - F_{xFL}\right) + \frac{T_W}{2} \cdot \left(F_{xRR} - F_{xRL}\right),\ u_2 = \delta \tag{7}$$

Thus the vehicle yaw dynamics can be reformulated as in the following

$$\dot{\omega}_z = \frac{a}{I_{zz}} \cdot \left(F_{yFL} + F_{yFR}\right) - \frac{b}{I_{zz}} \cdot \left(F_{yRL} + F_{yRR}\right) + \frac{1}{I_{zz}}u_1 + \frac{a \cdot \left(F_{xFL} + F_{xFR}\right) - \frac{T_W}{2} \cdot \left(F_{yFR} - F_{yFL}\right)}{I_{zz}}u_2 \tag{8}$$

When the tire slip angles are sufficiently small, this formulation can be approximated with

$$\dot{\omega}_z = \frac{bC_r - aC_f}{I_{zz}v_x}v_y - \frac{a^2C_f + b^2C_r}{I_{zz}v_x}\omega_z + \frac{1}{I_{zz}}u_1 + \frac{aC_f + a\cdot\left(F_{xFL}+F_{xFR}\right) - \frac{T_W}{2}\cdot\left(F_{yFR}-F_{yFL}\right)}{I_{zz}}u_2 \quad (9)$$

The design of the stabilization controller is founded on the multiple sliding surface control theory [8]. A sliding surface is first defined with respect to the sideslip velocity: $S_1 = x_1 - x_{1d}$. To make the surface attractive, one enforces $\dot{S}_1 = -k_1 S_1$, where k_1 is a positive convergence rate. Substitute vehicle lateral dynamics and replace the unknowns with their estimated versions, one obtains the yaw rate command.

$$\bar{x}_2 = \frac{\left(\hat{F}_{yFL}+\hat{F}_{yFR}\right)+\left(\hat{F}_{yRL}+\hat{F}_{yRR}\right)}{Mv_x} + \frac{\left(\hat{F}_{xFL}+\hat{F}_{xFR}\right)}{Mv_x}\delta + \frac{k_1 v_y}{v_x} \quad (10)$$

To avoid directly differentiating tire forces, the yaw rate command $\bar{x}_2$ is filtered by a first-order lag to generate the desired yaw rate x_{2d} obeying $\tau\cdot\dot{x}_{2d} + x_{2d} = \bar{x}_2$, where the time constant τ is a design parameter.

A second sliding surface is then defined for the yaw rate convergence: $S_2 = x_2 - x_{2d}$. Similarly, to make the surface attractive, one imposes $\dot{S}_2 = -k_2 S_2$, where k_2 is also a positive convergence rate. After substitutions, the desired yaw moment and steering angle can be computed by

$$u_{1d} = -a\cdot\left(\hat{F}_{yFL}+\hat{F}_{yFR}\right) + b\cdot\left(\hat{F}_{yRL}+\hat{F}_{yRR}\right) - \left[a\cdot\left(\hat{F}_{xFL}+\hat{F}_{xFR}\right) - \frac{T_W}{2}\cdot\left(\hat{F}_{yFR}-\hat{F}_{yFL}\right)\right]\hat{u}_2 + I_{zz}\left[\dot{x}_{2d} - k_2\left(x_2 - x_{2d}\right)\right] \quad (11)$$

$$u_{2d} = \frac{I_{zz}}{aC_f + a\cdot\left(\hat{F}_{xFL}+\hat{F}_{xFR}\right) - \frac{T_W}{2}\cdot\left(\hat{F}_{yFR}-\hat{F}_{yFL}\right)} \times \left[-\left(\frac{bC_r - aC_f}{I_{zz}v_x}v_y - \frac{a^2C_f + b^2C_r}{I_{zz}v_x}\omega_z + \frac{1}{I_{zz}}\hat{u}_1\right) + \dot{x}_{2d} - k_2\left(x_2 - x_{2d}\right)\right] \quad (12)$$

The side of differential braking solely depends on the sign of the yaw moment command u_{1d}. As for the magnitude, if the desired yaw moment is achievable, the braking pressure commands are computed through the linearized gains from pressures to braking forces. If the requested braking pressures are too large, the front outside wheel will be allowed to be locked up (λ = -100%), and the rear outside wheel will be subject to a wheel-slip control mode. A desired wheel slip λ_d is chosen so that adequate braking and cornering forces are maintained. At actuator level, sliding mode wheel-slip control [9] is implemented to execute the regulation task.

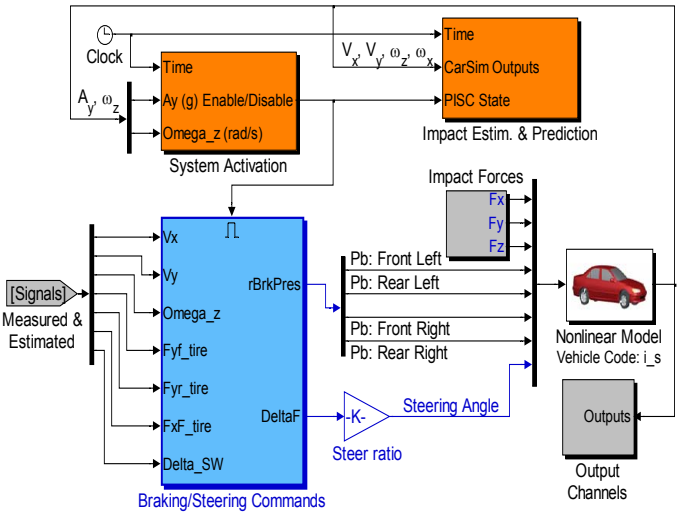

Fig. 4. Simulation architecture of the control system.

The overall system structure is modularized. It consists of three major subsystems as illustrated in Fig. 4: system activation and de-activation, impact estimation and prediction, as well as the generation of braking and steering commands. The vehicle dynamics model in the form of a CarSim S-function takes external impact forces, four wheel-cylinder pressures, as well as steering wheel angle as inputs, and generates an array of variables for analysis and visualization.

IV. Simulation Results

To evaluate the effectiveness of the proposed control system, simulations are performed to compare vehicle motions with various post-impact safety measures. The simulated collision has a generic layout illustrated in Fig. 5, in which colliding vehicles are "freed" to highlight the collision impulses. The road is straight and its adhesion condition is homogeneous with coefficient μ_R = 0.70. Both vehicles have parameters corresponding to the "baseline big SUV" dataset used in CarSim (M = 2450 kg, a = 1.105 m, b = 1.745 m, h_{CG} = 0.66 m, I_{zz} = 4946 kg-m^2, etc).

It is assumed both the target (Vehicle 1) and the bullet (Vehicle 2) vehicles are traveling along their own longitudinal axes when the collision occurs, with v_{1x} = 29 m/s (104 km/h, or 65 mph), v_{2x} = 33.5 m/s (120 km/h, or 75 mph), and their initial lateral velocities, yaw rates, and roll rates are all zero. The target vehicle is aligned with road tangent, whereas the bullet vehicle has an orientation angle θ_2 = 25°. At the instant of crash, the impact location on the bullet vehicle is at the center of its front bumper, whereas the location on the target vehicle is 0.1 m to the left of its rear bumper center. The coefficient of restitution (e) is assumed to be 0.20 for this angled rear-end crash.

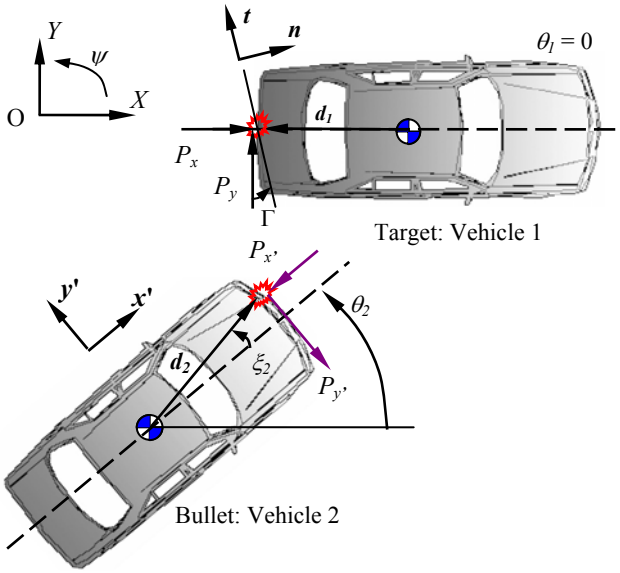

Fig. 5. An angled rear-end collision scenario.

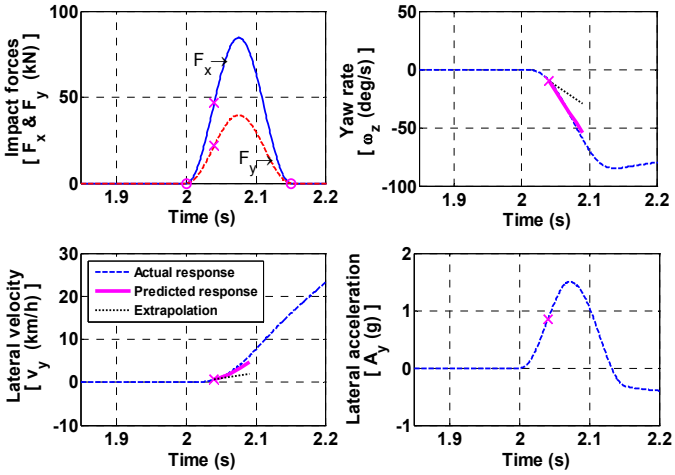

Fig. 6. Comparison of actual and predicted dynamic responses of the struck vehicle in an impact.

Fig. 6 presents the results of impact detection and validation for the target vehicle. The impact starts at time instant 2 second and lasts for a duration of 0.15 second. However, this crash is not sensed until the time instant at 2.04 second, which is marked by the crosses in all subplots. The predictions of the yaw rate and the lateral velocity are computed with the estimated impulse and a nominal four-DOF vehicle model as in Section II, and plotted with solid lines. In contrast, the linearly extrapolated results from the yaw rate and the lateral velocity at three latest sampling times are shown in the hidden lines. It is evident that the trend of the predicted response is consistent with that of the actual measurements, and it is unlikely that this increasing trend is purely caused by a sensor malfunction, noises, or the driver's aggressive maneuvers. Therefore, the detected impact is validated and confirmed.

Fig. 7 shows a comparison of the trajectories for four vehicles subject to the same impulsive disturbance, but with different control approaches. In each case, the space between two horizontal dashed lines represents one traffic lane.

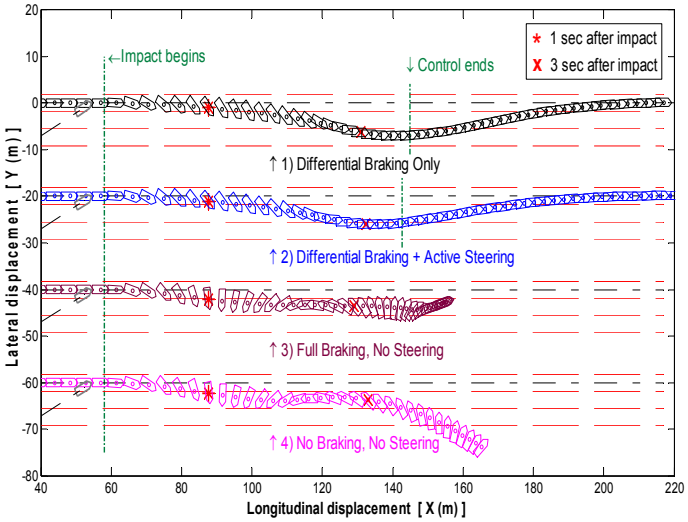

Fig. 7. Comparison of vehicle trajectories subject to the same impulsive disturbance with various control approaches.

Without the intervention of control systems or by the driver (Case 4), the peak post-impact yaw rate can reach −89°/s, and the vehicle develops a substantial lateral velocity. It keeps spinning and skidding until its kinetic energy is consumed by the ground resistance forces.

In the "full braking no steering" scenario (Case 3), maximum ABS-regulated braking is applied to all the wheels as soon as the impact is detected. Although the longitudinal velocity is reduced, the yaw rate decays in an uncontrolled way and the vehicle still spins around.

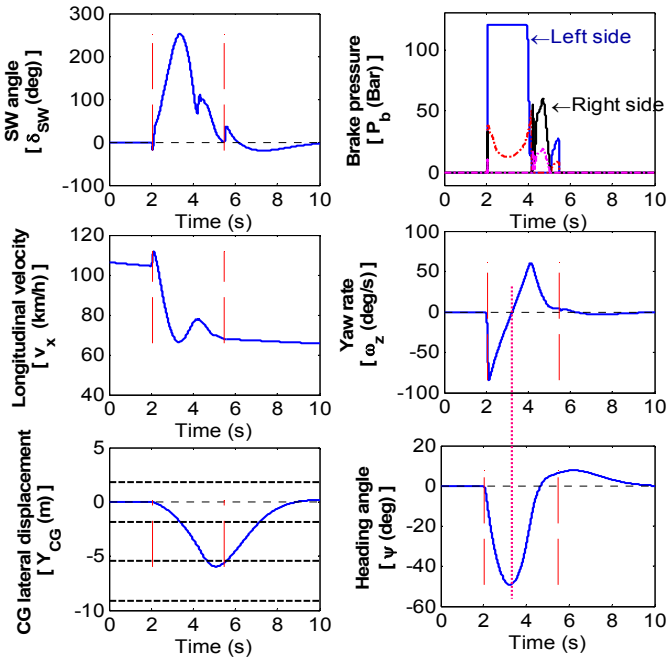

Fig. 8. Inputs and outputs of the target vehicle with the control system.

The benefits provided by the proposed system are demonstrated in Case (2). Time responses of the major inputs

and outputs are shown in Fig. 8. The collision triggers the crash sensing scheme and the control system is activated within the time interval from 2.05 second to 5.48 second, which is delimited by vertical dashed lines in subplots. It is further assumed that the driver takes over the control authority as soon as the control system is de-activated, because the yaw rate and lateral acceleration of the vehicle have been mitigated to the level that a normal driver can handle comfortably. The driver model smoothly steers the vehicle back to its original course, and eventually yaw rate, lateral velocity, lateral displacement, and heading angle all converge to zero. Case (1) in Fig. 7 shows that if active front steering is not available, most benefits in vehicle stabilization can still be maintained. The primary reason is when tire slip angles are too large, the control authority of steering is dramatically reduced due to tire force saturation [10].

In a larger context, the effectiveness of the proposed system is evaluated with an array of angled rear-end collision scenarios (Fig. 9). The collision conditions are similar to the one illustrated in Fig. 5, except for varying pre-impact bullet vehicle velocity ($v_{2x'}$ = 32~35 m/s) and angle (θ_2 = 15~30°), which can generate post-impact yaw rate up to -125°/s. The yaw rate mitigation criteria are defined in Eq. (13) and have a scale of 0 to 100. It is a quantitative measure of how much disturbance-induced yaw rate can be alleviated within one second after the event.

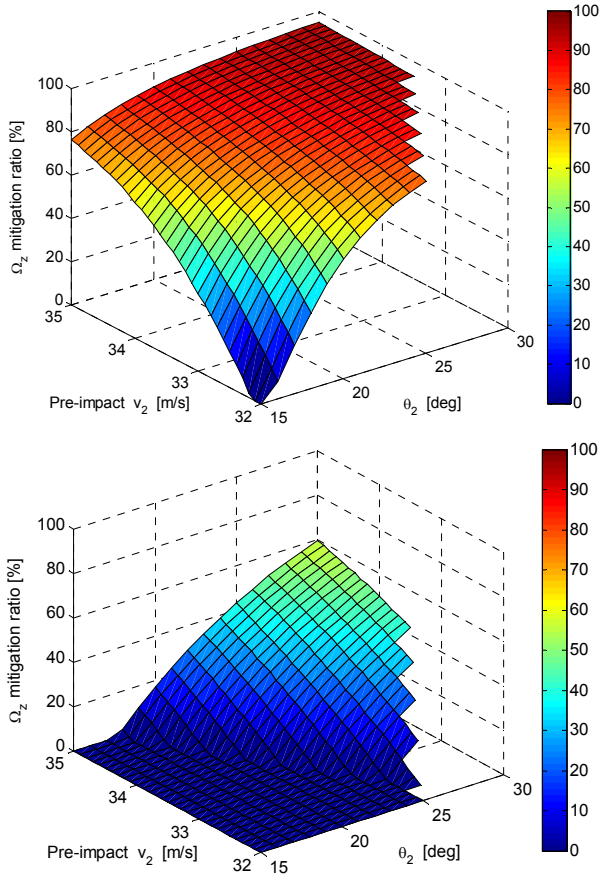

Fig. 9. Yaw rate mitigation ratios with 4-wheel braking (top) and differential braking (bottom) for the target vehicle in angled collisions.

$$\Omega_z\% = \frac{\min\left(\left|\Omega_z\right|_{t\in[t_0+0.1,\, t_0+1]}\right)}{\max\left(\left|\Omega_z\right|\right)} \times 100\% \tag{13}$$

For the case with 4-wheel full braking (top subplot of Fig. 9), although distinct mitigation can be observed for less severe situations, it is still inadequate in most extreme cases. For the proposed system (bottom subplot), the yaw rate can be successfully mitigated, and in many situations the value is zero, which means the heading angles have stopped building up and start to decline.

V. Conclusions

In this investigation, we proposed a vehicle stabilization control system in response to the exogenous impulsive disturbance. A crash sensing and validation scheme is first devised to activate the control system. Then a stabilization algorithm based on the sliding surface control is developed to attenuate the post-event vehicle motions. The effectiveness of the proposed system is demonstrated in CarSim simulation environment. In a generic angled rear-end collision scenario, the post-event vehicle stability can be recovered effectively, compared with the approach of automatic full braking on four wheels. Further work regarding the interaction of existing ESC and the proposed system will be reported in the next phase. In addition, the robustness of the crash detection scheme and the stabilization controller requires further examination.

Acknowledgment

Authors thank the constructive inputs from Bengt Jacobson at Volvo Car Corp. and Daniel Eisele at Ford North America.

References

[1] NHTSA: Traffic Safety Facts 2006. NHTSA Report DOT HS 810 818 (2008).

[2] Langwieder, K., Sporner, A., Hell, W.: RESICO – Retrospective Safety Analysis of Car Collisions Resulting in Serious Injuries. GDV 9810, Munich, Germany (1999).

[3] Chan, C.-Y. and Tan, H.-S.: Feasibility Analysis of Steering Control as a Driver-Assistance Function in Collision Situations. IEEE Trans. on Intelligent Transportation Systems, 2 (1), pp. 1–9 (2001).

[4] More safety in accidents: Secondary Collision Mitigation from Bosch. Retrieved August 06, from http://www.bosch-presse.de (2007).

[5] Thor, M.: The Efficiency of Electronic Stability Control after Light Collisions, Master's Thesis, Chalmers University of Technology, Goeteborg, Sweden (2007).

[6] Zhou, J., Peng, H., and Lu, J.: Collision Model for Vehicle Motion Prediction after Light Impacts, Vehicle System Dynamics, Vol. 46, Supplement 1, pp. 3–15 (2008).

[7] Gillespie, T.D.: Fundamentals of Vehicle Dynamics. Society of Automotive Engineers, Warrendale, PA (1992).

[8] Hedrick, J.K. and Yip, P.P.: Multiple Sliding Surface Control: Theory and Application, ASME Journal of Dynamic Systems, Measurement and Control, 122, pp. 586–593 (2000).

[9] Bang, M.S., Lee, S.H., Han, C.S., Maciuca, D.B. and Hedrick, J.K.: Performance Enhancement of a Sliding Mode Wheel Slip Controller by the Yaw Moment Control. Proc. ImechE, Vol. 215, Part D, pp. 455–468 (2001).

[10] Shibahata, Y., Shimada, K., Tomari, T.: Improvement of Vehicle Maneuverability by Direct Yaw Moment Control, Vehicle System Dynamics, 22, pp. 465–481 (1993).